ACS OMEGA

http://pubs.acs.org/journal/acsodf

Article

Activated Carbon Produced from the Hydrothermal Treatment of Glucose with KOH Activation for Catalytic Absorption of CO_2 in a BEA-AMP Bi-Solvent Blend

Foster Amoateng Appiah, Dzifa Nugloze, Lois Sandra Sai-Obodai, Paweesuda Natewong, and Raphael O. Idem*

Cite This: *ACS Omega* 2023, 8, 9346−9355

Read Online

ACCESS | Metrics & More | Article Recommendations

ABSTRACT: The amine-based postcombustion CO_2 capture (PCC) process involves absorption of CO_2 into a solvent and then regenerating the solvent to produce CO_2. In this study, the effect of an activated carbon (AC) catalyst, synthesized through hydrothermal treatment and furnace activation on CO_2 absorption in a 4M BEA/AMP amine blend, was evaluated and compared with that of a KMgO/CNTs (1:4) catalyst. The physical and chemical properties of AC were investigated with a scanning electron microscope (SEM), CO_2 temperature-programmed desorption (CO_2-TPD), Brunauer−Emmett−Teller (BET), powder X-ray diffraction (XRD), and thermogravimetric analyzer (TGA) and compared with the KMgO/CNTs (1:4) catalyst. The results showed that when compared against noncatalytic CO_2 absorption, AC enhanced the linear rate of CO_2 absorption by 33.3%, while for KMgO/CNTs, it was reported as 25.5%. The relatively higher surface area, combined with the higher number and strength of basic sites of AC relative to the KMgO/CNTs (1:4) catalyst, provided effective basic reaction sites for CO_2 absorption, thereby enhancing the rate of CO_2 absorption into the amine. AC was also relatively easier to synthesize which would provide a good replacement for the CNT-based catalyst which has carcinogenic tendencies.

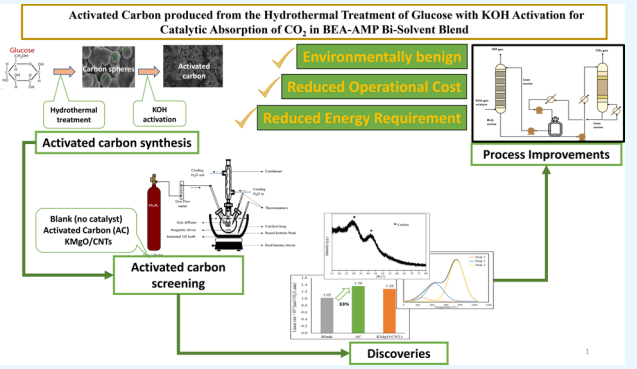

1. INTRODUCTION

In recent years, many countries have been striving to ensure that global warming is limited to less than 2 °C, preferably 1.5 °C, relative to preindustrial levels.[1] CO_2 capture technology has received much of the attention because it is the major and most abundant greenhouse gas (GHG) that contributes to the devastating effects of climate change caused by global warming.[2] About 35 billion tons of CO_2 are reported to have been released into the atmosphere in 2019 alone, with the energy sector being the major contributor.[3] CO_2 capture technologies mainly include postcombustion capture, precombustion capture, and oxy-fuel combustion. Of these three, the postcombustion CO_2 capture technology is reported to be the most mature.[4]

The amine-based postcombustion CO_2 capture technology involves the use of amine or reactive solvents to selectively capture CO_2 from the flue gas by an absorption process. In this process, the CO_2 reacts chemically with the amine, and is then regenerated in a desorber column and the CO_2 recovered. The main factors to be considered for a successful operation of the amine-based postcombustion CO_2 capture process are the reaction kinetics, CO_2 absorption capacity, the regeneration energy requirement, as well as solvent degradation, solvent corrosiveness, and solvent foaming. Some extensively used conventional amines include monoethanolamine (MEA), diethanolamine (DEA), and methyldiethanolamine (MDEA), but over the years, these amines have been found to have some limitations including low solvent stability, corrosiveness, slow kinetics, low absorption capacity, low thermal stability, and high energy requirements which constitute the bottleneck of this technology. Researchers have sought to remedy these limitations by exploring other amines. The type and placement of the functional groups within the amine structure immensely affect its performance.[5−7] To achieve both high thermodynamic absorption capacity and fast desorption rates, steric hindrance, which affects the basicity of the amines, and the

Received: December 5, 2022
Accepted: February 14, 2023
Published: February 28, 2023

formation of carbamate and bicarbonate ions is a major factor for aqueous amino alcohol solutions as this directly influences CO_2 capture performance.[8] A blend of different amines where one of the amines is preferably sterically hindered, has been suggested to address some of the limitations, specifically desorption kinetics and solvent regeneration energy.[9−11] Narku-Tetteh et al.[6] developed a criterion for selection of components for formulation of amine blends based on structure−activity relationships of different types of amines.

In addition to the search for the best amine and optimum blends for the process, the use of a solid catalyst has been introduced into the amine-based postcombustion CO_2 capture process. The use of a solid acid catalyst in desorption was first introduced by Idem et al.[12] to aid in the reduction of the high energy requirements of the amine-based postcombustion CO_2 capture technology by enhancing the rate of desorption.[12] For the absorption process, the enhanced kinetics is achieved by the introduction of a solid base catalyst into the system. A base is defined as a proton acceptor by Bronsted-Lowry theory, and an electron-pair donor by Lewis theory. These definitions of a base are essential in understanding the role of a porous solid base catalyst in the absorption process. The absorption reaction of CO_2 and an aqueous amine solution can be described using a widely accepted "zwitterion reaction mechanism".[13] The mechanism involves two steps, which are the transfer of electrons from the amine molecule to the CO_2 molecule to form the zwitterion intermediate followed by the second step, which is the deprotonation of the zwitterion intermediate to form a stable carbamate. The zwitterion formation step is considered as the rate-determining step (RDS).[14] A Lewis base catalyst having a stronger alkalinity than that of the amine thus releases their electrons to the CO_2 ahead of the amine in the first step which helps to facilitate the subsequent reaction between CO_2 and the amine to occur much more easily, resulting in a faster system kinetics. On the other hand, a Bronsted-Lowry base catalyst aids in the second step which involves the deprotonation of the zwitterion intermediate. An additional benefit of the catalyst is that it provides a large interfacial area for reaction of CO_2 and amine to occur, thus enhancing mass transfer of the absorption reaction. Researchers have reported the use of many basic catalysts for the amine-based postcombustion CO_2 capture process.[15−17] Carbon-based materials such as activated carbon, carbon nanofibers, and carbon nanotubes (CNTs) are considered very good materials due to their large surface area and high-electron-density surface for facilitating the gas absorption reaction.[18,19]

In recent studies by Natewong et al.,[16] CNTs were prepared using chemical vapor deposition of methane (CH_4) and CO_2 over a Ni/MgO catalyst. They tested various catalysts consisting of CNTs, K/MgO,[15] and their mixtures in different ratios in an amine-based postcombustion CO_2 system. Their studies revealed that a mixture of CNTs and K/MgO resulted in very-high-performance catalysts for CO_2 absorption with a BEA−AMP solvent, with the best mixing ratio being 1:4 (KMgO/CNTs).[16] However, concerns about the toxicity and preparation cost of CNTs begs the need for the development of other catalyst options.[20,21] Recent studies have revealed that carbon nanotubes (CNTs) are carcinogenic and have dire health concerns.[22−24] An alternative carbon-based catalyst reported in the literature with a high surface area is carbon spheres. Carbon spheres have been reported in the literature to be synthesized by the Stöber method, chemical vapor deposition (CVD), and hydrothermal treatment.[25−28] Though there are extensive literature studies on the synthesis and characterization of carbon spheres and their applications in CO_2 adsorption, not much has been reported on the use of carbon spheres in amine-based postcombustion CO_2 capture. This work seeks to synthesize activated carbon (AC) using the hydrothermal treatment of the glucose method followed by furnace activation with KOH and characterization for a comparative study on:

1. The preparation procedure of AC against that of KMgO/CNTs to ascertain the optimum catalyst in terms of ease of preparation and overall safety.
2. Absorption performance of AC against that of KMgO/CNTs (1:4) in a 4M BEA-AMP bisolvent blend amine system.

2. EXPERIMENTAL SECTION

2.1. Materials and Equipment. Butylethanolamine (BEA, ≥98%, Sigma-Aldrich), 2-amino-2-methyl-1-propanol (AMP, ≥98%, Sigma-Aldrich), hexamethylenediamine (HMDA, ≥98%, Sigma-Aldrich), and branched-polyethylenimine (PEI, M_w 800, Sigma-Aldrich), glucose ($C_6H_{12}O_6$, Sigma-Aldrich), potassium hydroxide (KOH, 85%, Alfa Aesar), premixed gas (15% CO_2, balance N_2, Praxair Canada), hydrochloric acid for titrations (HCl, 1 N, Sigma-Aldrich), catalyst binder (LUDOX AM colloidal silica, 30 wt % suspension in H_2O), pH test strips (Micro Essential Laboratory), dual hot plate/stirrer (Fisher Scientific Company), flow meter (Electronic AALBORG GFM171, ±1% accuracy), FEI Nova NanoSEM 450 Scanning Electron Microscope equipped with an Everhart Thornley detector (ETD), Bruker D8 Advance ECO instrument, TA Instruments SDT Q600 and TG-DTG, Micromeritics 3Flex Surface Analyzer, and ChemBET 3000 TPR/TPD instrument.

2.2. Synthesis of Activated Carbon Sphere (ACS). Glucose solution, a precursor for the AC catalyst, was prepared by completely dissolving 100 g of glucose in 200 mL of distilled water. The glucose solution was then transferred into a 250 mL Teflon-lined stainless-steel autoclave reactor and placed in a preheated oven maintained at 190 °C for 24 h for the hydrothermal treatment. After the hydrothermal treatment, the autoclave reactor was cooled to room temperature, and a dark-brown solid product (carbon spheres) was extracted from the autoclave. It was washed with distilled water until the pH of the filtrate was approximately 7, confirmed by pH indicator strips. The washed carbon spheres were dried overnight in an oven at 110 °C. KOH solution (1 g of KOH in 1.5 mL of water) was prepared and mixed with the washed carbon spheres obtained after drying, in a mass ratio of 1:4 carbon spheres to KOH. The mixture was then dried overnight at 110 °C. The solid mixture was crushed into powder after drying and activated at 600 °C for 2 h in a furnace. After activation, the product was washed with distilled water until the pH of the filtrate was approximately 7. The activated carbon catalyst obtained was dried overnight at 110 °C and finally pelletized to obtain particle sizes in the range of 4.2 to 4.7 mm.

2.3. Synthesis of Carbon Nanotubes-K/MgO. The procedure for the synthesis of carbon nanotubes (CNTs)-K/MgO described in this section is based on what was reported by Natewong et al.[16] It involved physically mixing CNTs and K/MgO catalysts that were individually prepared. To obtain K/MgO, MgO powder obtained from the calcination of the precursor $Mg(OH)_2$ at 600 °C for 2 h, was impregnated with 1

https://doi.org/10.1021/acsomega.2c07758
ACS Omega 2023, 8, 9346−9355

mol % KOH solution, dried at 110 °C, and finally calcined at 600 °C for 2 h. The second component, CNTs, were prepared by the chemical vapor deposition method using a CH_4/CO_2 gas mixture as precursors over Ni/MgO support. Details of the preparation of both components are described elsewhere.[16]

2.4. Catalyst Characterization. The surface morphology of the raw carbon spheres (CS) as well as AC was examined using micrographs obtained from an FEI Nova NanoSEM 450 scanning electron microscope equipped with an Everhart Thornley detector (ETD).

A powder X-ray diffraction (PXRD) pattern for the AC catalyst was collected using a Bruker D8 Advance ECO instrument equipped with a Cu Kα source (λ = 1.54178 Å, kV = 40, mA = 25) and a LYNXEYE XE detector. Analysis parameter used was 2θ scans from 15−80°, with a step size of 0.02° and a scan rate of 2.5° per minute.

Thermogravimetric analysis (TGA) was performed by temperature-programmed oxidation in a TA Instruments SDT Q600. Approximately, 1.4 mg of powder sample was loaded into a blank ceramic sampler holder attached to the instrument balance. An air flow rate of 50 mL/min was used, and the TGA was performed from 30 to 900 °C with a heating rate of 10 °C/min.

The surface area, pore volume, and pore size were also determined using the Brunauer−Emmett−Teller (BET) method with data from a Micromeritics 3Flex Surface Analyzer. Prior to analysis, the catalyst was degassed under N_2 flow for 2 h at 200 °C using the Micrometrics VacPrep061. Analysis was then conducted at −196 °C in a Micromeritics 3Flex Surface Analyzer. The specific surface area of the catalyst was determined by N_2 adsorption/desorption.

The strength and number of basic sites that are known to have a strong correlation with the absorption enhancement performance of a catalyst were determined by CO_2-temperature-programmed desorption (CO_2-TPD) with a ChemBET 3000 TPR/TPD instrument. During measurement, 0.05 g of catalyst, placed in a quartz U-type glass reactor was degassed at 200 °C for 1 h under a helium flow of 60 mL/min to remove any air or physically adsorbed moisture. The catalyst was then cooled to room temperature followed by adsorption of 3% (v/v) CO_2/N_2 at a flow rate of 100 mL/min and a temperature of 40 °C for 1 h. After adsorption, the CO_2 was desorbed by a gradual increase in temperature from room temperature to 1050 °C with He gas at a flow rate of 60 mL/min as a carrier gas. The CO_2 desorbed was monitored using a thermal-conductivity detector.

2.5. Absorption Experiment. The absorption experiment was aimed at comparing the absorption performance of the new AC catalyst with KMgO/CNTs introduced by Natewong et al.[16] As a result, 4M BEA/AMP bisolvent blend was selected as the amine solvent, and a temperature of 40 ± 2 °C was used in all the absorption experiments. The choice of absorption conditions was based on the conditions employed in the work done by Natewong et al.[16] to obtain a fair basis to assess the performance of the new AC basic catalyst.

The CO_2 absorption experiment was conducted using the experimental setup as illustrated in Figure 1. The setup consists of a three-necked 250 mL round-bottom flask to accommodate a thermometer (on one neck), a condenser (on the middle neck), and a gas diffuser (on the other neck). These three components were used to monitor temperature, reduce amine losses through cooling, and disperse the CO_2 into the amine, respectively. 5 g of the actual catalyst (excluding binder) was

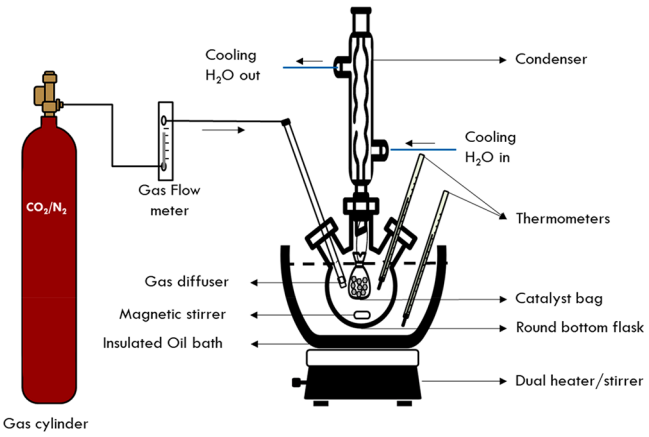

Figure 1. CO_2 absorption experimental set-up.

measured in a bag and attached to the middle neck of the flask to ensure full immersion of the catalyst in the amine solution. The flask with its components, supported by a clamp, was immersed in an oil bath mounted on a dual-purpose heater/stirrer during an experimental run. Another thermometer was used to monitor the temperature of the oil bath, and the gas diffuser was connected to a gas cylinder/supply. Prior to a typical run, the water cooler that feeds the condenser and an oil bath heater were engaged and set to supply cooling water at 5 ± 2 °C, and to maintain the oil bath at 40 ± 2 °C, respectively. The stirrer was also set to a constant speed of 600 rpm. The flask, with 100 mL of standard amine solution, a magnetic stirrer, and all neck connections in place (excluding the gas diffuser replaced with a cork) was gently immersed in the oil bath to heat it to the absorption temperature of 40 ± 2 °C. Once the amine solution reached the desired temperature, the gas diffuser connected to a premixed gas tank (15% CO_2 with N_2 balance) and set at a flow rate of 200 mL/min (±2 accuracy) was placed in the flask to start bubbling the CO_2 into the amine solution, which marked time 0 of the reaction. Using a 100−1000 micropipette, 1 mL of the amine was sampled at time intervals of 10 min (starting from time 0) for the first hour, 30 min interval up to the third hour, and then after an hour interval until the equilibrium was reached. Equilibrium was reached when the CO_2 loading was found to be constant. The Chittick apparatus based on the acid titration technique[16] was used to determine the CO_2 loading of the samples. Plots of CO_2 loading against time were generated for the blank and catalytic runs, and the linear absorption rates were estimated from the slope of the linear portion of the absorption profiles. The absorption experiment was conducted more than three times, and the average deviation of repeatability was below 1%. The operating conditions for these screening experiments are summarized in Table 1.

3. RESULTS AND DISCUSSION

3.1. Catalyst Characterization. Figure 2 (a) and (b) show the SEM images of carbon spheres (CS) after hydrothermal treatment and AC after furnace activation with KOH respectively. The micrograph of CS showed that large quantities of solid carbon spheres with spherical surface morphologies were formed during the hydrothermal treatment. However, it can be observed that the carbon spheres were partially fused together. These observations were consistent with those reported by other studies that synthesized CS from

https://doi.org/10.1021/acsomega.2c07758
ACS Omega 2023, 8, 9346−9355

Table 1. Summary of Operating Conditions for the Screening Experiments

parameter	value	unit
Gas flow rate	200 ± 2	mL/min
Gas composition	15% CO_2, N_2 balance	
Absorption temperature	40 ± 2	°C
Solvent volume	100	ml
Catalyst weight	5	g
Stirring speed	600	rpm
Amine solvent	4M BEA/AMP	

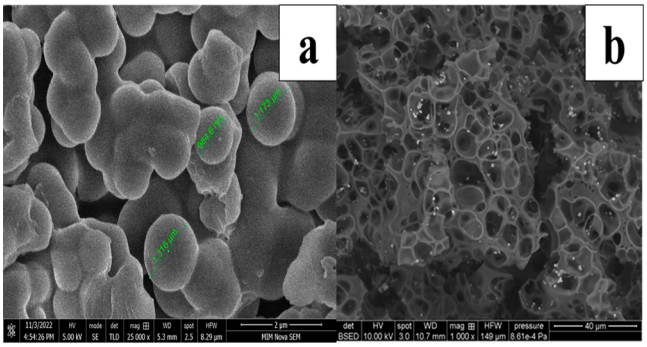

Figure 2. SEM images of (a) raw carbon sphere (CS) after hydrothermal treatment (b) AC, after furnace activation with KOH.

various carbon sources,[29−31] which proves that the dark brown solid residue obtained from the hydrothermal treatment of glucose was carbon spheres. The micrograph of AC shows what appears to be cavities of different sizes on the surface of the carbon creating a highly porous and broad surface. Comparatively, it can be deduced that the KOH activation of CS enhanced the surface area and pore volume by leaching gaseous carbon-based surface compounds from the K−C molecules formed during the activation.[32]

The phase composition of the AC catalyst which is indicated by the XRD pattern is shown in Figure 3. From the XRD pattern, two broad peaks at 2θ of 29.2° and 42.6° which correspond to reflections of amorphous carbon were observed.[16,28,33] Similar broad amorphous carbon reflections were reported by researchers including the reference work for

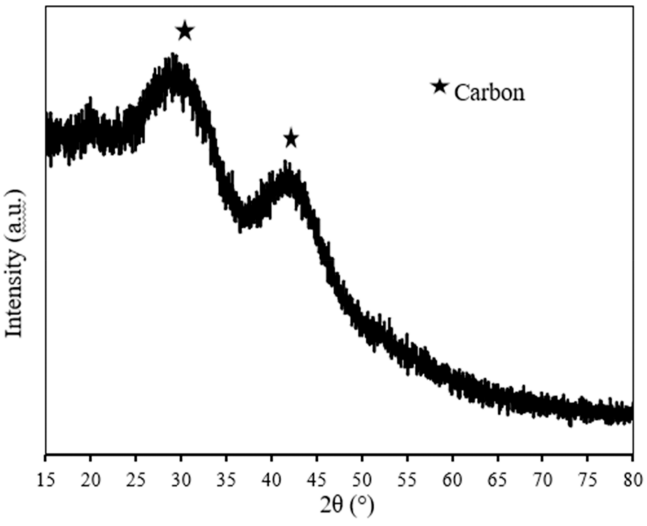

Figure 3. XRD pattern of AC.

KMgO/CNTs. The absence of a K peak in the XRD pattern may be due to its concentration being below the detection limit of the analysis technique used.

The thermogravimetric analysis (TGA) representing the weight-loss curve of AC is provided in Figure 4. From the

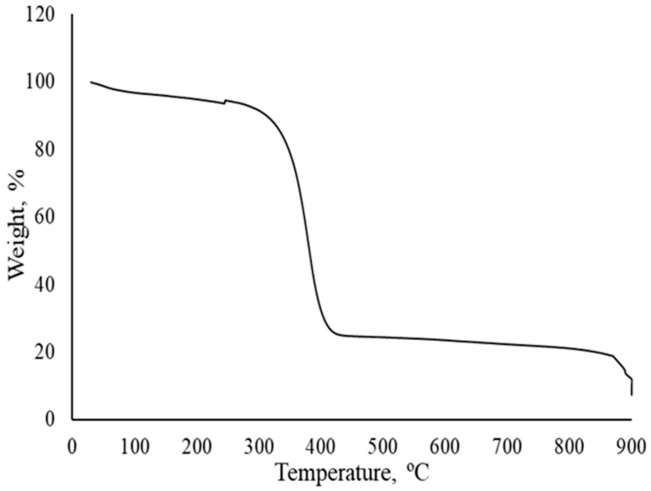

Figure 4. TGA graph of AC.

curve, the thermal stability and the composition of the catalyst can be determined. From the weight loss analysis, the AC catalyst sample was composed mainly of C (87.1%) with some amounts of volatile matter (5.4%) and inorganic content (7.5%).

The surface area, pore volume, as well as pore size distribution of the AC catalyst were estimated with data obtained from a Micromeritics 3Flex Surface Analyzer using the Brunauer−Emmett−Teller method. The results are listed in Table 2. Additionally, the BET analysis on KMgO/CNTs

Table 2. BET Surface Area and Porosity Analysis of the Catalysts

catalyst	surface area (m^2/g)	pore volume (cm^3/g)	average pore size (nm)
AC	839.4	0.484	2.31
KMgO/CNTs	107.4	0.479	5.90

catalyst obtained by Natewong et al.[16] are also included in Table 2. From the data, it was observed that AC has a larger surface area of 839.4 m^2/g compared to 107.4 m^2/g recorded for KMgO/CNTs, while similar pore volumes were obtained for the two catalysts. The superior surface area observed for AC is consistent with the general literature studies.[26,30,34] In contrast to the surface areas, KMgO/CNTs recorded a larger average pore size distribution of 5.90 nm relative to 2.31 nm measured on AC.

The basicity analysis, including the number and strength of basic sites in the catalyst, were quantified by integrating the CO_2-TPD profiles obtained from the ChemBET 3000 TPR/TPD instrument. Natewong et al.,[16,35] Afari et al.,[15] and Narku-Tetteh et al.[36] have established that basicity characteristics of the solid absorber catalyst have a considerable influence on the performance of catalyzed amine-based CO_2 absorption. Generally, desorption peak with temperature near the range of 50 to 250 °C represents basic sites with weak

https://doi.org/10.1021/acsomega.2c07758
ACS Omega 2023, 8, 9346−9355

strength while peak within temperature ranges of 250 to 650 °C and at higher temperature (above 650 °C) corresponds to basic sites with medium and strong strengths respectively, on the catalyst. The CO_2-TPD profile graph along with the number of basic sites obtained from CO_2-TPD analysis are reported in Figure 5 and Table 3 respectively. As shown in

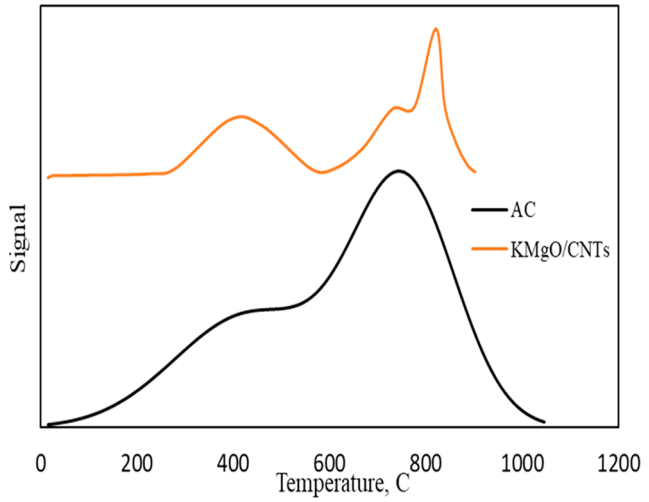

Figure 5. CO_2-TPD profile of AC and KMgO/CNTs catalysts.

Table 3. Basic Sites Characteristics of the Catalysts

catalyst	weak sites (mmol CO_2/g)	medium sites (mmol CO_2/g)	strong sites (mmol CO_2/g)	total sites (mmol CO_2/g)
AC	0.049	0.424	0.655	1.128
KMgO/CNTs	–	0.238	0.594	0.832

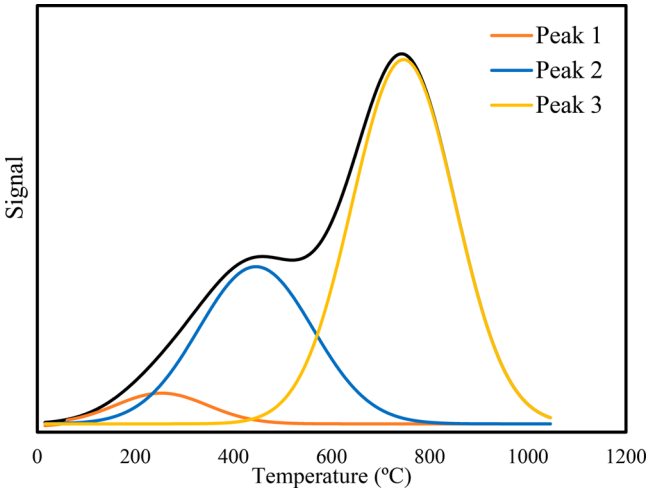

Figure 6. Deconvoluted CO_2-TPD profile of AC catalyst.

Figure 6, three deconvoluted CO_2 desorption peaks at peak temperatures of 233, 437, and 754 °C representing the presence of weak, medium, and strong basic sites respectively were observed for AC catalyst. On the other hand, the study of Natewong et al.[16] showed that medium and strong basic sites were also observed on KMgO/CNTs. However, as seen from the data in Table 3, the numbers of weak, medium, and strong basic sites combined to total basic sites (obtained by integration of the desorption peaks) measured are higher in AC than that of the KMgO/CNTs catalyst.

3.2. Catalyst Screening. *3.2.1. Rate of Absorption.* The reaction between amines, particularly primary and secondary amines, with CO_2 is described by the generally accepted Zwitterion mechanism. It includes a two-step process characterized by the formation of intermediate in step 1 and the consequent breakdown to form stable carbamate and protonated amine in step 2. However, some structural effects such as the steric hindrance effect typically leads to the formation of unstable carbamates which are in turn hydrolyzed to bicarbonate and free amine.[8,37] For the BEA-AMP system, during the absorption reaction, BEA being a secondary amine reacts with CO_2 to form stable carbamates, whereas the steric character of AMP leads to bicarbonate formation through hydrolysis of carbamate. The reactive absorption between the BEA/AMP solvent used and CO_2[15] is illustrated below.

Step 1: Zwitterion formation

$$BEA + CO_2 \rightarrow BEA^+COO^- \quad (R1)$$

$$AMP + CO_2 \rightarrow AMP^+COO^- \quad (R2)$$

Step 2: Formation of carbamate and protonated amine

$$BEA^+COO^- + BEA \rightarrow BEACOO^- + BEA^+ \quad (R3)$$

$$AMP^+COO^- + AMP \rightarrow AMPCOO^- + AMP^+ \quad (R4)$$

Hydrolysis of unstable carbamate of AMP to bicarbonate is given by

$$AMP^+COO^- + H_2O \rightarrow AMP^- + CO_2 + H_2O \quad (R5)$$

$$AMP^- + CO_2 + H_2O \rightarrow AMP + HCO_3^- \quad (R6)$$

3.2.1.1. Linear Absorption Rate. The screening results were expressed in a key performance parameter which is the linear CO_2 absorption rate, obtained from the linear portion of the CO_2 absorption profiles. The role of the catalyst in the amine-based CO_2 absorption is to speed up the rate at which the amine takes up CO_2 by providing more active reaction sites. This was achieved through the added interactive surface area and basic sites provided by the catalyst.

The absorption screening experiment data constituted three different systems: the blank (without catalyst) and the two catalytic systems (AC and KMgO/CNTs). At the end of each screening experiment, an absorption profile which indicates the CO_2 loading of the solvent as a function of the reaction time was generated. Generally, the profile consists of two parts: the linear section and the section where it tapers off. The slope of the linear section of the profile is used to determine the linear CO_2 absorption rate, whereas the tapering section usually indicates the absorption characteristic as the system approaches equilibrium.

The CO_2 absorption profiles obtained from the batch-scale screening experiment for the blank and AC systems were compared with that reported by Natewong et al.[16] for KMgO/CNTs in Figure 7. From the graph, it was observed that the absorption profiles for the AC and KMgO/CNTs systems were above the blank system as anticipated.

The effect of the AC catalyst on the absorption kinetics of the 4M BEA/AMP was evaluated in this study and compared with the activity of the KMgO/CNTs (1:4) catalyst as reported by Natewong et al.[16] Evidently, the linear rate of

https://doi.org/10.1021/acsomega.2c07758
ACS Omega 2023, 8, 9346−9355

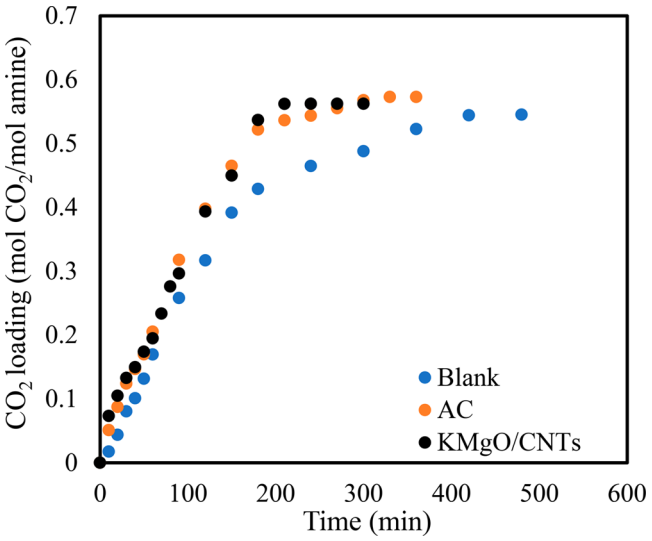

Figure 7. CO_2 absorption profiles of 4M BEA/AMP at 40 °C with a gas rate of 200 mL/min (blank and catalytic systems).

absorption data in Figures 8 and 9 show that both catalytic systems recorded faster kinetics compared to the blank system.

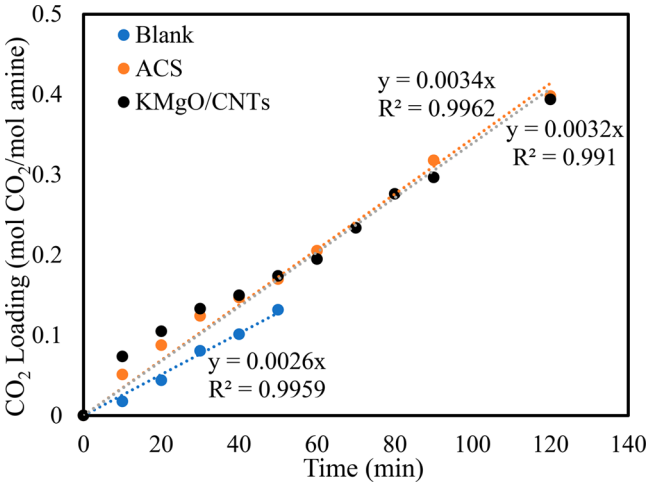

Figure 8. Linear section of CO_2 absorption profiles for 4M BEA/AMP biblend at 40 °C with a gas rate of 200 mL/min (blank and catalytic systems).

A linear rate of absorption of 1.02 ($\times 10^{-2}$ mol CO_2/Lsoln·min) was recorded for the blank system in this work, which is consistent with 1.00 ($\times 10^{-2}$ mol CO_2/Lsoln·min) recorded by Narku-Tetteh et al.[6] for the same 4M BEA/AMP system. This validates the accuracy and consistency of the rate obtained in this study. The linear rate obtained for the KMgO/CNTs catalyst run was 1.28 ($\times 10^{-2}$ mol CO_2/Lsoln·min), while the linear rate obtained for the AC catalyst was 1.36 ($\times 10^{-2}$ mol CO_2/Lsoln·min). Based on this, the rate activity of the KMgO/CNTs catalyst corresponds to a percentage enhancement of 25.5% in reference to the blank run. Regarding the AC catalyst, its rate relative to the blank translates to a substantial percentage enhancement of 33.3%. From the above, it can be established that the CO_2 absorption rate activity of the AC catalyst was higher than that of KMgO/CNTs. In summary, the linear absorption rate of CO_2 ranks in the increasing order of blank < KMgO/CNTs < AC.

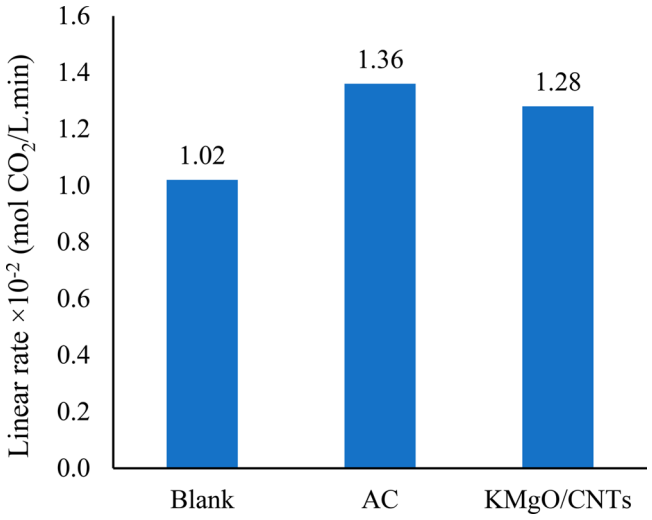

Figure 9. Linear absorption rate of 4M BEA/AMP biblend at 40 °C with a gas rate of 200 mL/min for blank and catalytic systems.

From the CO_2-TPD results obtained in Table 3, AC had a higher total number of basic sites, about 36% more basic sites than KMgO/CNTs, which means it had more active sites to aid the capture of the CO_2 gas. In addition to this higher number of basic sites, the total surface area of the AC catalyst was about eight (8) times higher than that of KMgO/CNTs with a slightly higher pore volume as well. This observation indicates that a higher degree of dispersion of the active basic sites were achieved, thus making the active basic sites of AC catalyst more accessible as compared to the KMgO/CNTs catalyst. The combination of the higher strength and total number of basic sites (chemical property) and higher surface area (physical property) accounts for the relatively higher absorption rate of AC compared with KMgO/CNTs. This supports and proves the fact that both the chemical and physical properties of a catalyst are important in enhancing the absorption kinetics in a catalytic system, though their contribution may not be equal. The higher total surface area means there is a greater number of available crystallite area for amine and CO_2 to interact.

3.2.1.2. Initial Absorption Rate Based on Pseudo First Order Kinetics. Following the power law, the rate of reaction between CO_2 and the amine solvent is equal to the product of the reaction constant, k, and the concentrations of the reactants raised to their stoichiometric coefficients. This is given by eq 1. In the system studied, the concentration of the amine solvent is fairly constant for the duration of the experiment with the help of the condenser attached to the reaction vessel. This means that the concentration term with respect to the amine is constant and can be merged with k. This makes the rate equation dependent on C_A as shown in eq 2.

$$\text{rate} = kC_A^n C_B^m \quad (1)$$

$$\text{rate} = k_1 C_A^n \quad (2)$$

C_A is the concentration of CO_2 within the amine in the reaction vessel that acts as a driving force of the reaction and pushes the CO_2 loading from zero at the start of the reaction to the equilibrium loading obtained at the end of the reaction. One way to express the driving force, C_A, is by taking the difference between the maximum concentration at equilibrium,

https://doi.org/10.1021/acsomega.2c07758
ACS Omega 2023, 8, 9346−9355

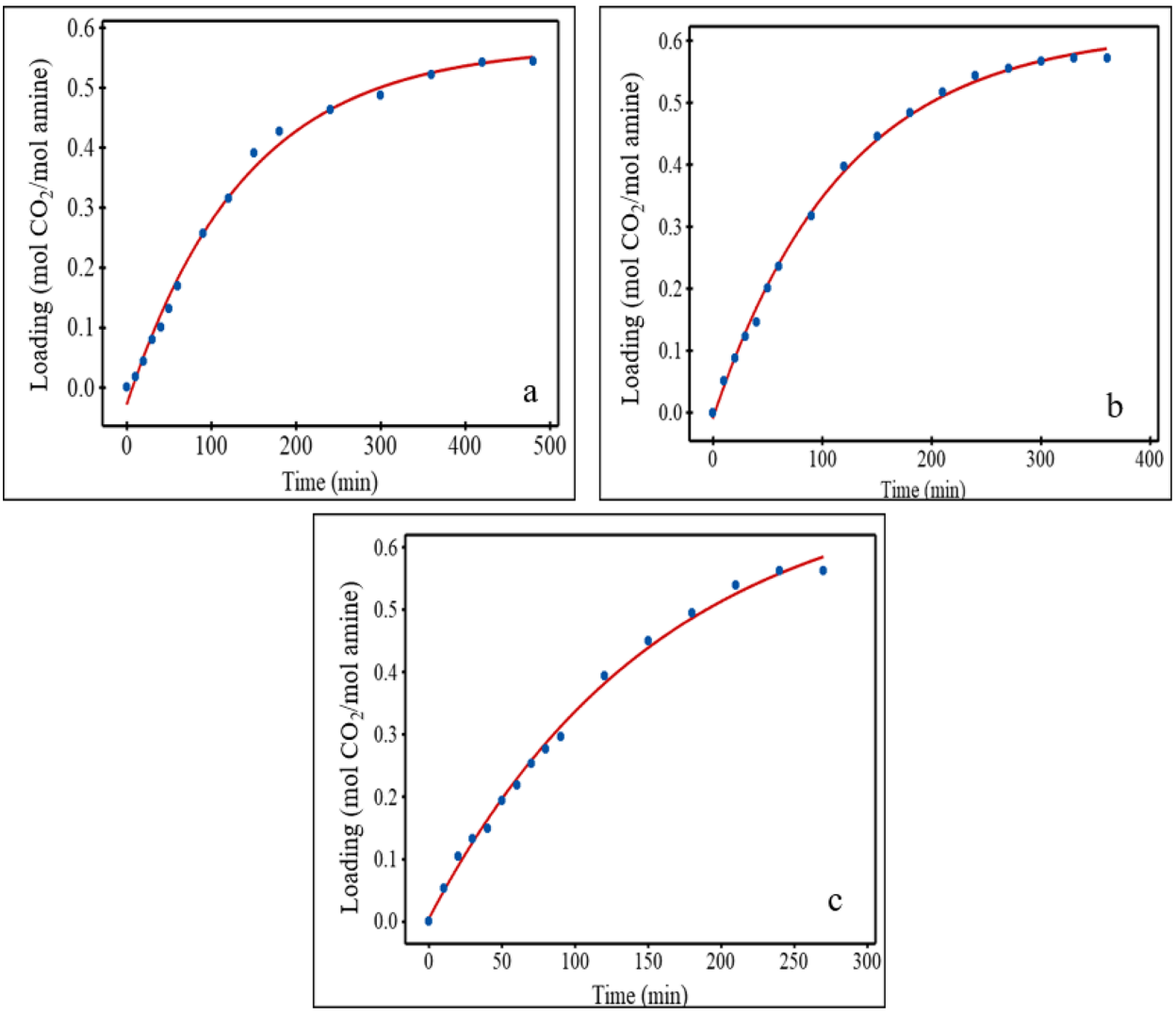

Figure 10. Nonlinear regression plots of CO_2 loadings against time for 4M BEA/AMP biblend at 40 °C with a gas rate of 200 mL/min (a: blank; b: AC; c: KMgO/CNTs).

C_{Amax} and the concentration at any time during the reaction, C_{At} as shown in eq 3.[15,38,39]

$$\text{rate} = k_1(C_{Amax} - C_{A,t})^n \quad (3)$$

To determine the rate of the reaction based on eq 3, that is, the initial rate based on pseudo-first order reaction, the reaction constant was determined using the CO_2 loading against time profiles obtained from the screenings shown in Figure 7. These profiles were fitted using nonlinear regression models of Minitab software to obtain equations that correspond to the plots. Figure 10 shows the fitted models obtained for the blank, AC, and KMgO/CNTs runs, respectively. The obtained equations were then differentiated to obtain the rate expression for the three systems from which rate values at each sampling time were calculated. For monoamines reacting with CO_2 as is the case of the systems studied, $n = 1$.[39] A plot of rate against $(C_{Amax} - C_A)$ was generated to calculate the reaction constant, k_1, which was the slope of the plot shown in Figure 11 for each system. With k_1 calculated, the initial absorption rates based on pseudo-first order reaction for the blank, AC and KMgO/CNTs systems were calculated and compared in Figure 12. The values obtained showed an enhancement of approximately 30% for

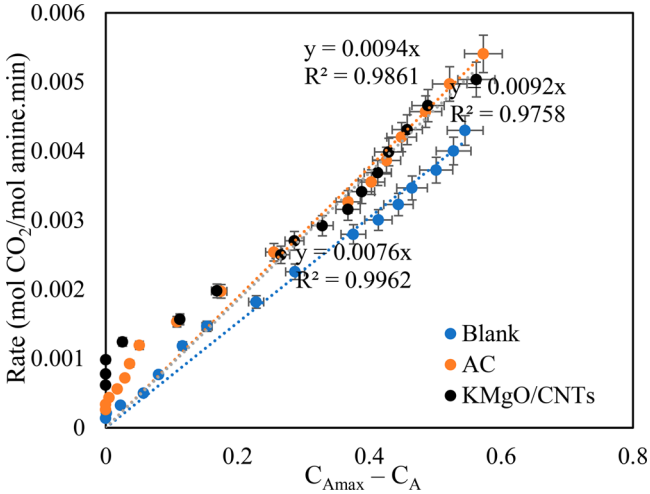

Figure 11. Plots of rate against $C_{Amax} - C_A$ for 4M BEA/AMP biblend at 40 °C with a gas rate of 200 mL/min for the blank and catalytic systems.

AC and 25% for KMgO/CNTs relative to the blank system. These relative percentage enhancements are similar to the

https://doi.org/10.1021/acsomega.2c07758
ACS Omega 2023, 8, 9346−9355

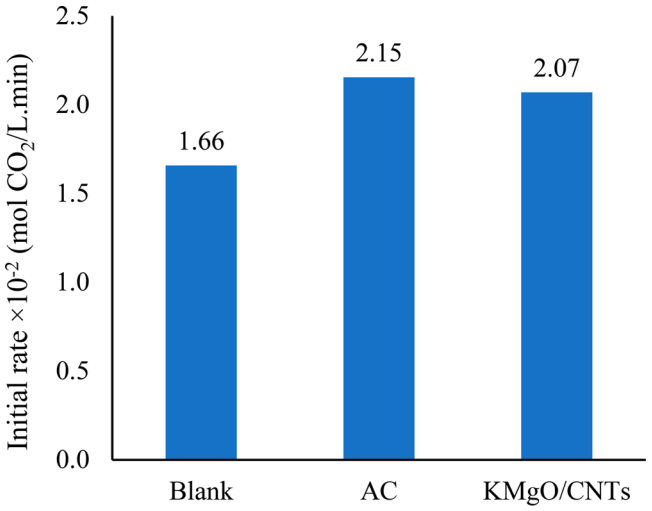

Figure 12. Initial absorption rate (based on pseudo-first order kinetics) of 4M BEA/AMP biblend at 40 °C with a gas rate of 200 mL/min for blank and catalytic systems.

trend observed for the linear absorption rate assessment. It was also determined that the percentage deviation obtained for comparing the initial rates based on pseudo-first order approximations with the actual initial rates based on the obtained regression model was less than 3%. This means that the pseudo-first order approximations were appropriate for the system studied. Table 4 compares all the different rates that were estimated in this study.

Table 4. Different Rate Types Estimated for Blank and Catalytic Systems Studied

		initial absorption rate (× 10^{-2} mol CO_2/min·L)		
catalyst	linear rate (× 10^{-2} mol CO_2/min·L)	actual	pseudo-first order	deviation, %
blank	1.02	1.71	1.66	2.9
AC	1.36	2.16	2.15	0.5
KMgO/CNTs	1.28	2.01	2.07	3.0

3.3. Equilibrium Loading. Equilibrium loading can be defined as the maximum amount of CO_2 any amine can hold at equilibrium. This amount is mainly dependent on the solubility of CO_2 in the amine and is affected by the absorption temperature, CO_2 partial pressure, and amine concentration. Within the constraints of a practical run time, the theoretical loading is never achieved, and hence the equilibrium loading is better appreciated. The theoretical CO_2 loading of a solvent can be determined by the stoichiometric reaction equation of the solvent and CO_2 and is always higher than its equilibrium loading. A catalyst is employed to shorten the time needed to reach the equilibrium loading. The introduction of absorption catalyst accelerates the absorption reaction and should not affect the equilibrium of the reaction. The catalyst will only push the absorption of CO_2 to reach equilibrium faster than the conventional reaction carried out without one. This can be clearly seen from the data in Figure 7 as the AC system approached the thermodynamic equilibrium within a relatively shorter time of 300 min compared to 360 min in the blank system. In essence, the presence of the AC catalyst resulted in achieving equilibrium loading faster as against the blank, confirming the inability to achieve the theoretical CO_2 loading of 1 mol CO_2/mol amine for BEA/AMP solvent in practice. (The slight difference of 0.03 mol CO_2/mol amine in equilibrium loading between the catalytic system and the blank could be because of the minor variations in operating conditions such as room temperature, pressure, humidity etc. or minor variance in the experimental setup due to human interference.)

3.4. Validation of AC Performance. Having confirmed the superior performance of AC in BEA/AMP, further screening was conducted with 2M HMDA/PEI solvent, a novel solvent blend considered for the CO_2 capture process. This was to confirm the performance of the AC catalyst in other solvents to establish its absorption performance with any selected amine solvent. 2M HMDA/PEI blank absorption run was compared with the catalytic run with AC as the catalyst in the system. The linear profiles and linear rate of absorption for both runs are shown in Figures 13 and 14 respectively.

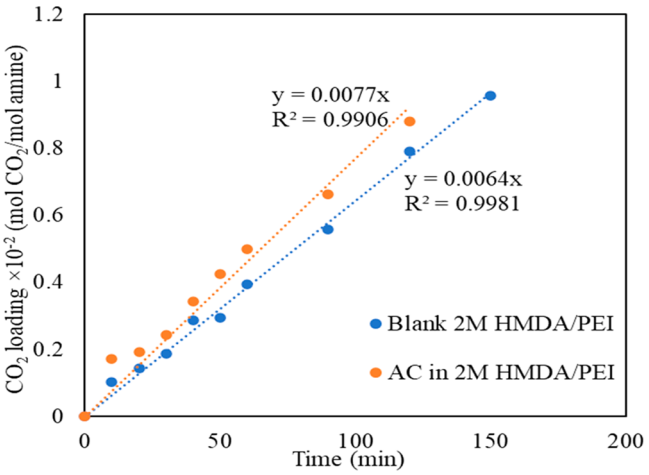

Figure 13. Linear profile of 2M HMDA/PEI at 40 °C with a gas rate of 200 mL/min for AC and blank systems.

The introduction of the AC catalyst enhanced the linear rate of absorption by 21% relative to the blank. This enhanced performance can be attributed to the combined effect of the

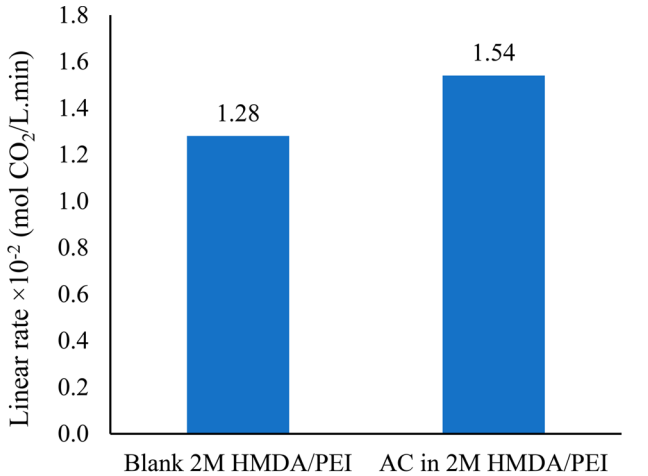

Figure 14. Linear rate of absorption of 2M HMDA/PEI at 40 °C with a gas rate of 200 mL/min for AC and blank systems.

https://doi.org/10.1021/acsomega.2c07758
ACS Omega 2023, 8, 9346−9355

physical and chemical properties of AC, with the physical properties, mainly its high surface area, pore volume, and pore size playing a bigger role. Thus, the high surface area, pore volume, and pore size made the active sites of the catalyst easily accessible, hence the observed increase in the linear rate of reaction. The strength and number of basic sites, which represents the chemical property of AC, also showed that AC was able to donate electrons, which is required in the rate-determining step for the amine-CO_2 reaction mechanism. The availability of extra electrons due to the presence of the AC catalyst explains the increased rate in the catalytic run as compared to the blank run.

Thus, with the runs involving HMDA/PEI, the absorption performance of the AC catalyst was confirmed, and it can be said that the observed superior performance over KMgO/CNT makes it a suitable choice for an absorber catalyst irrespective of the selected amine solvent.

3.5. Comparison of AC and KMgO/CNTs Preparation Methods and Safety. From the synthesis procedures described for AC and KMgO/CNTs in the Experimental Section, a comparison was done to ascertain which of these two catalysts is easier and safer to synthesize. In relation to safety, there have been concerns raised about the carcinogenic potential of CNTs and its implications to the environment, which was one of the driving factors for an alternative catalyst.[22−24] AC has no such concerns making it a preferred option for safe operations. In addition, a thorough analysis of the synthesis procedures of both catalysts revealed that KMgO/CNTs preparation was much more complex and more costly compared to that of AC. This on a large scale translates into higher production time and cost, making AC a preferred catalyst.

4. CONCLUSIONS

The objective of synthesizing, characterizing, and screening of a new absorber catalyst, AC, has been achieved. The performance of the AC catalyst was compared to KMgO/CNTs, an existing catalyst and was found to be superior. The AC catalyst showed a 33.3% enhancement in the linear absorption rate with BEA/AMP, whereas KMgO/CNTs showed a 25.5% enhancement of the linear absorption rate, relative to the BEA/AMP blank. This superior performance of AC was found to be a combination of both its physical and chemical properties. The higher surface area of the AC catalyst as compared to KMgO/CNTs increased the number of exposed active sites for the BEA/AMP-CO_2 reaction, whereas the stronger and higher number of basic sites made more electrons readily available for the deprotonation of the zwitterion intermediate, which is the rate-determining step in the absorption kinetics of the amine-CO_2 reaction.

In addition, the AC catalyst was validated using HMDA/PEI biblend solvent confirming its ability to enhance the absorption rate in the capture process irrespective of the amine solvent. The introduction of AC also serves as a good replacement to KMgO/CNTs since CNTs have been found to be carcinogenic. Thus, the AC catalyst is a more environmentally friendly absorber catalyst.

It will be however recommended that further studies be employed on how to increase the yield of the AC catalyst for large scale application. Also, the fine particles of the AC catalyst made the pelletizing process a bit challenging. An improved pelletizing process to obtain pellets that are stable and resistant to wear and tear would be advantageous to increase the potentials of AC as an absorber catalyst.

AUTHOR INFORMATION

Corresponding Author

Raphael O. Idem − *Clean Energy Technology Research Institute (CETRI), Faculty of Engineering and Applied Science, University of Regina, Regina, Saskatchewan S4S 0A2, Canada*; orcid.org/0000-0002-2708-0608; Phone: +1-306-585-4470; Email: raphael.idem@uregina.ca; Fax: +1-306-585-4855

Authors

Foster Amoateng Appiah − *Clean Energy Technology Research Institute (CETRI), Faculty of Engineering and Applied Science, University of Regina, Regina, Saskatchewan S4S 0A2, Canada*

Dzifa Nugloze − *Clean Energy Technology Research Institute (CETRI), Faculty of Engineering and Applied Science, University of Regina, Regina, Saskatchewan S4S 0A2, Canada*

Lois Sandra Sai-Obodai − *Clean Energy Technology Research Institute (CETRI), Faculty of Engineering and Applied Science, University of Regina, Regina, Saskatchewan S4S 0A2, Canada*

Paweesuda Natewong − *Clean Energy Technology Research Institute (CETRI), Faculty of Engineering and Applied Science, University of Regina, Regina, Saskatchewan S4S 0A2, Canada*

Complete contact information is available at: https://pubs.acs.org/10.1021/acsomega.2c07758

Notes

The authors declare no competing financial interest.

ACKNOWLEDGMENTS

The work was financially supported by the SaskPower Clean Energy Research Chair (SCERCh) program at the University of Regina, Clean Energy Technology Research Institute (CETRI) and the Natural Science & Engineering Research Council of Canada (NSERC).

REFERENCES

(1) *The Paris Agreement*; UNFCCC, 2015.

(2) *Climate Change 2014: Synthesis Report. Contribution of Working Groups I, II and III to the Fifth Assessment Report of the Intergovernmental Panel on Climate Change*; IPCC, 2014; p 151.

(3) Ritchie, H.; Roser, M. *CO_2 and Greenhouse Gas Emissions*; OurWorldInData.org, https://ourworldindata.org/co2-and-greenhouse-gas-emissions, 2020.

(4) Law, L. C.; Yusoff, A. N.; Abd, S. S. R. Optimization and economic analysis of amine-based acid gas capture unit using monoethanolamine/methyldiethanolamine. *Clean Technol. Environ. Policy* **2018**, *20*, 451−461.

(5) Xiao, M.; Liu, H.; Idem, R.; Tontiwachwuthikul, P.; Liang, Z. A study of structure-activity relationships of commercial tertiary amines for post-combustion CO_2 capture. *Appl. Energy* **2016**, *184*, 219−29.

(6) Narku-Tetteh, J.; Muchan, P.; Saiwan, C.; Supap, T.; Idem, R. Selection of components for formulation of amine blends for post combustion CO_2 capture based on the side chain structure of primary, secondary and tertiary amines. *Chem. Eng. Sci.* **2017**, *170*, 542.

(7) Muchan, P.; Saiwan, C.; Narku-Tetteh, J.; Idem, R.; Supap, T.; Tontiwachwuthikul, P. Screening tests of aqueous alkanolamine solutions based on primary, secondary, and tertiary structure for

https://doi.org/10.1021/acsomega.2c07758
ACS Omega 2023, 8, 9346−9355

blended aqueous amine solution selection in post combustion CO_2 capture. *Chem. Eng. Sci.* **2017**, *170*, 574−82.
(8) Sartori, G.; Savage, D. W. Sterically hindered amines for carbon dioxide removal from gases. *Ind. Eng. Chem. Fundam.* **1983**, *22*, 239−49.
(9) Adeosun, A.; Abu-Zahra, M. Evaluation of amine-blend solvent systems for CO_2 post-combustion capture applications. *Energy Procedia* **2013**, *37*, 211−218.
(10) Chakravarty, T.; Phukan, U. K.; Weilund, R. H. Reaction of acid gases with mixtures of amines. *Chem. Eng. Prog.* **1985**, *81*, 4.
(11) Nwaoha, C.; Supap, T.; Idem, R.; Saiwan, C.; Tontiwachwuthikul, P.; AL-Marri, M.; Benamor, A. Advancement and new perspectives of using formulated reactive amine blends for post-combustion carbon dioxide (CO_2) capture technologies. *Petroleum* **2017**, *3*, 10−36.
(12) Idem, R.; Shi, H.; Gellowitz, D.; Paitoon, T. Catalytic method and apparatus for separating a gaseous component from an incoming gas stream, WO2011120138A1, 2011.
(13) Crooks, J. E.; Donnellan, J. P. Kinetics and mechanism of the reaction between carbon dioxide and amines in aqueous solution. *J. Chem. Soc., Perkin Trans.* **1989**, *2*, 331−333.
(14) Caplow, M. Kinetics of carbamate formation and breakdown. *J. Am. Chem. Soc.* **1968**, *90*, 6795−803.
(15) Afari, D. B.; Coker, J.; Narku-Tetteh, J.; Idem, R. Comparative kinetic studies of solid absorber catalyst (K/MgO) and solid desorber catalyst (HZSM-5)-aided CO_2 absorption and desorption from aqueous solutions of MEA and blended solutions of BEA-AMP and MEA-MDEA. *Ind. Eng. Chem. Res.* **2018**, *57*, 15824−39.
(16) Natewong, P.; Prasongthum, N.; Reubroycharoena, P.; Idem, R. Application of carbon nanotubes prepared from CH_4/CO_2 over ni/MgO catalysts in CO_2 capture using a BEA-AMP bi-solvent blend. *Clean Energy* **2019**, *3*, 251−262.
(17) Shi, H.; Naami, A.; Idem, R.; Tontiwachwuthikul, P. Catalytic and non catalytic solvent regeneration during absorption-based CO_2 capture with single and blended reactive amine solvents. Int. *J. Greenhouse Gas Control* **2014**, *26*, 39−50.
(18) Khalil, S. H.; Aroua, M. K.; Daud, W. M. A. W. Study on the improvement of the capacity of amine-impregnated commercial activated carbon beds for CO_2 adsorbing. *Chem. Eng. J.* **2012**, *183*, 15.
(19) Lu, C.; Bai, H.; Wu, B.; Su, F.; Hwang, J. F. Comparative study of CO_2 capture by carbon nanotubes, activated carbons and zeolites. *Energy Fuels* **2008**, *22*, 3050−6.
(20) Kobayashi, N.; Izumi, H.; Morimoto, Y. Review of toxicity studies of carbon nanotubes. *J. Occup. Health* **2017**, *59*, 394−407.
(21) Francis, A. P.; Devasena, T. Toxicity of carbon nanotubes: a review. *Toxicol Ind. Health* **2018**, *34*, 200−10.
(22) Barbarino, M.; Giordano, A. Assessment of the carcinogenicity of carbon nanotubes in the respiratory system. *Cancers (Basel)* **2021**, *13*, 1318.
(23) Orsi, M.; Al Hatem, C.; Leinardi, R.; Huaux, F. Carbon nanotubes under scrutiny: their toxicity and utility in mesothelioma research. *Appl. Sciences* **2020**, *10*, 4513.
(24) Toyokuni, S. Genotoxicity and carcinogenicity risk of carbon nanotubes. *Adv. Drug Deliv Rev.* **2013**, *65*, 2098−2110.
(25) Liu, J.; Qiao, S. Z.; Liu, H.; Chen, J.; Orpe, A.; Zhao, D.; Lu, G. Q. Extension of the stöber method to the preparation of monodisperse resorcinol-formaldehyde resin polymer and carbon spheres. *Angewandte Chemie - International Edition* **2011**, *50*, 5947−5951.
(26) Li, M.; Li, W.; Liu, S. Hydrothermal synthesis, characterization and KOH activation of carbon spheres from glucose. *Carbohydr. Res.* **2011**, *346*, 999−1004.
(27) Li, M.; Li, W.; Liu, S. Control of the morphology and chemical properties of carbon spheres prepared from glucose by a hydrothermal method. *J. Mater. Res.* **2012**, *27*, 1117−1123.
(28) Wickramaratne, N. P.; Jaroniec, M. Activated carbon spheres for CO_2 adsorption. *ACS Appl. Mater. Interfaces* **2013**, *5*, 1849−1855.
(29) Mi, Y.; Hu, W.; Dan, Y.; Liu, Y. Synthesis of carbon microspheres by a glucose hydrothermal method. *Mater. Lett.* **2008**, *62*, 1194−1196.
(30) Tripathi, K. N. Porous carbon spheres: recent developments and applications. *AIMS Mater. Sci.* **2018**, *5*, 1016−1052.
(31) Jain, A.; Balasubramanian, R.; Srinivasan, M. P. Hydrothermal conversion of biomass waste to activated carbon with high porosity: a review. *Chem. Eng. Sci.* **2016**, *283*, 789−805.
(32) Tran, T. T. V.; Kongparakul, S.; Reubroycharoen, P.; Guan, G.; Nguyen, M. H.; Chanlek, N.; Samart, C. Production of furan-based biofuel with an environmental benign carbon catalyst. *Environ.l Prog. Sustainable Energy* **2018**, *37*, 1455−1461.
(33) Khalil, H. P. S.; Jawaid, M.; Firoozian, P.; Rashid, U.; Islam, A.; Akil, H. M. Activated carbon from various agricultural wastes by chemical activation with KOH: preparation and characterization. *J. Biobased Mater. Bioenergy* **2013**, *7*, 708−714.
(34) Romero-Anaya, A. J.; Ouzzine, M.; Lillo-Ródenas, M. A.; Linares-Solano, A. Spherical carbons: synthesis, characterization and activation processes. *Carbon (New York)* **2014**, *68*, 296−307.
(35) Natewong, P.; Prasongthum, N.; Reubroycharoen, P.; Idem, R. Evaluating the CO_2 capture performance using a BEA-AMP biblend amine solvent with novel high-performing absorber and desorber catalysts in a bench-scale CO_2 capture pilot plant. *Energy Fuels* **2019**, *33*, 3390−3402.
(36) Narku-Tetteh, J.; Afari, D. B.; Coker, J.; Idem, R. Evaluation of the roles of absorber and desorber catalysts in the heat duty and heat of CO_2 desorption from butylethanolamine-2-amino-2-methyl-1-propanol and monoethanolamine-methyldiethanolamine solvent blends in a bench-scale CO_2 capture pilot plant. *Energy Fuels* **2018**, *32*, 9711−26.
(37) Narku-Tetteh, J. Development of criteria for selection of components for formulation of amine blends based on structure and activity relationships of amines, and validation of formulated blends in a bench scale CO_2 capture pilot plant. *Master's Thesis, University of Regina*, 2017.
(38) Levenspiel, O. *Chemical Reaction Engineering*, 3rd ed.; John Wiley & Sons: New York, 1999.
(39) Li, J. Kinetic study of carbon dioxide and alkanolamines both in aqueous and non-aqueous solutions using the stopped flow technique. Master's Thesis, University of Regina, 2007.

https://doi.org/10.1021/acsomega.2c07758
ACS Omega 2023, 8, 9346−9355